Article

Optimization of a Reverse Osmosis Desalination and Indirect Ocean Capture for a Polygeneration System

Maxine Camille O. Mallari [1,2], and Aristotle T. Ubando [1,2,3,*]

[1] Department of Mechanical Engineering, De La Salle University, 2401 Taft Avenue, Manila 0922, Philippines
[2] Thermomechanical Analysis Laboratory, De La Salle University, Laguna Campus, LTI Spine Road, Laguna Blvd., Biñan, Laguna 4024, Philippines
[3] Center for Engineering and Sustainable Development Research, De La Salle University, 2401 Taft Avenue, Manila 0922, Philippines
* Correspondence: aristotle.ubando@dlsu.edu.ph
Received: 29 April 2025; Revised: 4 September 2025; Accepted: 5 September 2025; Published: 10 September 2025

Abstract: With increasing carbon dioxide emissions from power and heat generation, various decarbonization strategies are being explored to produce clean energy. Polygeneration systems are a promising approach to supply the energy needed. These systems incorporate numerous processes and technologies to convert various raw materials into multiple energy streams. To capitalize on the vast ocean resources worldwide, reverse osmosis desalination (ROD) and indirect ocean capture (IOC) technologies are considered within polygeneration system. This study focuses on optimizing an ROD/IOC process unit incorporated in a polygeneration system that produces heating, cooling, purified water, and hydrochloric acid (HCl) according to demand. The optimization approach employs a mixed integer linear programming (MILP) model that considers net output, capacity, demand, and binary variable vectors. The model aims to maximize the profit while minimizing the carbon-associated price. The optimal results indicate the selection of a combined heat and power (CHP) unit operating at 7500 kW, the chiller at 1500 kW, the reverse osmosis desalination (ROD) unit at 130.5 tons per hour, and the electrolytic cell with a gaseous diffusion anode (EGDA) operating at 80 tons per hour. The system achieves a net positive profit between €447,000 to €4,691,000 per year depending on the carbon-associated price. A trade-off between the profitability and the carbon-associated price was established. This study contributes to the field of negative emission technologies (NETs) and emphasizes the importance of optimizing polygeneration systems for sustainable energy transition.

Keywords: polygeneration; desalination; optimization; low-carbon emissions; profitability; carbon-associated price

1. Introduction

Carbon dioxide (CO_2) and greenhouse gas emissions are a growing global concern as new industries and technologies continue to penetrate the market. Since the industrial revolution in the 1950s, a significant and rapid trend has been observed. In 2023, annual CO_2 emissions from fossil fuels and industry reached 37.79 billion tons worldwide [1]. Since 2002, atmospheric CO_2 concentrations increased from 365 ppm to 420 ppm, demonstrating the environmental impact of anthropogenic activities tied to economic growth [2]. Hence, global leaders, scientists, and engineers investigate approaches to mitigate the increasing CO_2 emissions while meeting energy demands for economic development.

To achieve the 2050 net-zero goal, the concept of decarbonization and low-carbon technologies is introduced. Low-carbon technologies include renewable energy technologies that harness energy from solar, wind, hydro, and biomass sources. According to the International Energy Agency (IEA) [3], renewable energy has the potential to expand from 30% of the global electricity sector in 2023 to 46% in 2030. Through renewable energy adoption, reliance on carbon-based energy sources is reduced, thus promoting the transition to decarbonization as an industrial standard. Consequently, exploring novel low-carbon technologies further advances the net-zero agenda.

Negative emission technologies (NETs) represent scalable solutions aimed at removing CO_2 from the atmosphere. Each technology has distinct potential, costs, and maturity levels [4]. Indirect ocean capture (IOC), involving the integration of dilute alkaline streams into ocean waters, offers a promising method to counteract ocean acidification and to sequester carbon. This approach leverages the natural process of mineral dissolution to enhance ocean alkalinity [5]. However, the advantages offered by IOC can only be realized if the economic barriers

are addressed [6]. Davies et al. [7] explored the integration of a reverse osmosis desalination (ROD) and IOC to treat rejected brine for ocean alkalinity enhancement. An electrolytic cell with a gaseous diffusion anode (EGDA) was included for its negative emission potential and minimal ecological risk. Tan et al. [8] developed a polygeneration system integrating a ROD/IOC process with a combined cooling, heating, and power (CCHP) unit. Their study optimized the model to identify the unit capacities based on demand, profit, and CO_2 emissions.

Polygeneration systems fulfill demands beyond energy production alone. These systems offer significant advantages in energy efficiency, cost-effectiveness, and environmental impact reduction [9]. Optimization of these systems maximizes their benefits by fine-tuning system components and operational strategies to achieve desired outcomes. Through optimization, one study presented a 15.4% improvement in system efficiency and a 7.1% reduction in product costs [10]. Similarly, an optimized decision support system for a polygeneration system achieved annual emission savings of 20% to 27% compared to a reference system [11]. Optimization techniques enable polygeneration systems to adapt to changing operational conditions, ensuring reliable operation and preventing system failure [11].

Mixed integer linear programming (MILP) is a common optimization technique for identifying optimal operation conditions for specific objectives. The MILP method is useful when the optimization problem considers binary or integer variables and linear constraints [12]. The MILP approach guarantees global optimality and can be solved efficiently using commercially available solvers. Consequently, MILP has been applied in various fields, particularly in energy and production systems [13]. MILP shows an especially promising application for negative emissions and polygeneration systems [14].

Studies have investigated the optimization of polygeneration systems and negative emissions. A Scopus keyword search for “polygeneration”, “desalination”, and “optimization” conducted on August 19, 2025, returned only 49 articles and one review paper, indicating potential research gaps in the literature. MILP demonstrated near-optimal solutions for achieving negative carbon footprint in biochar systems [15]. A MILP input-output model explored carbon dioxide removal through enhanced weathering in integrated polygeneration systems [16]. MILP was utilized to determine optimal operating capacities for technologies in polygeneration systems with desalination process [8]. Existing works focus on maximizing profit, reducing annual costs, or minimizing carbon emissions as the single-objective function, but rarely address multi-objective optimization criteria. Given the limited literature on desalination in polygeneration systems, this paper proposes a multi-objective function for an ROD/IOC-integrated polygeneration system, specifically for maximizing profitability and minimizing carbon emissions.

One common technique for multi-objective MILP is the weighted sum method, which assigns each objective a weight coefficient reflecting its importance. This method often yields a linear relationship between objectives [17]. It has been applied in diverse contexts: Olabi et al. [18] optimized a hydrogen supply chain considering cost, environmental impact, and safety using analytic hierarchy process (AHP) and technique for order of preference by similarity to ideal solution (TOPSIS) for weight determination; Cheng et al. [19] improved scheduling of an energy-aware manufacturing system based on makespan, energy consumption, and sharing costs; and Yilmaz and Yagmahan [20] optimized electric vehicle charging strategies to minimize costs and travel time. These studies demonstrate the capabilities of the weighted sum for multi-objective optimization problems.

Thus, the main research objective of the study is to select technologies and their operating capacities for a polygeneration system with a desalination process. The specific objective is to identify the scenario for maximizing the annual profitability and minimizing the carbon-associated price. These objectives are considered in a case study carried out by Tan et al. [8].

2. Mixed Integer Linear Programming Model

The mixed integer linear programming (MILP) model was selected for this optimization problem. The model was coded in LINGO 21.0.37 software and solved using a laptop with the following processor specifications: Intel® Core™ i5-8265U CPU @ 1.60 GHz, 1800 Mhz, 4 Core(s), 8 logical processors.

2.1. Model Formulation

Equation (1) shows the MILP model based on the classical generic process synthesis for maximum profit, developed by Grossmann and Santibanez and defined as the annual profit of process synthesis [21]. The parameters include the price vector (c_1), variable cost vector (c_2), fixed cost vector (c_3), and annualizing factor (AF). The decision variables included are the net output vector (y), capacity vector (x), and binary decision vector (b). The subsequent considerations and constraints discussed for the polygeneration system, represented by Equation (2), are adapted from the generic model. The model of the study maximizes annual profit, computed as the net stream revenue (NSV) minus annualized capital and operational costs (ACC).

$$\text{maximize } c_1^T y - AF(c_2^T x + c_3^T b) \tag{1}$$

where

$$\text{maximize } Profit = NSV - ACC \tag{2}$$

$$NSV = AWH(c_1^T y) \tag{3}$$

$$ACC = AF(c_2^T x + c_3^T b) \tag{4}$$

The net stream revenue (*NSV*), shown in Equation (3), is computed by taking the annual sales of products and by-products minus the cost of raw materials. The annual working hours (*AWH*) parameter is equal to 8000 h per year. The *ACC* refers to the fixed costs of technologies used and the variable costs of operations that are dependent on the product demands, as shown in Equation (4). The annualizing or capital recovery factor (*AF*) is set at 0.08.

To incorporate carbon-associated prices expressed in Equation (5), the objective function of maximizing profit in Equation (2). is adjusted to account for carbon emissions produced in the system and its costs. When minimizing the carbon-associated price, the objective function considers the tons of CO_2 produced per year. Since carbon production is usually measured in tons or parts per million of CO_2, a carbon coefficient is established to relate carbon production to annual profitability and costs. Equation (6) represents the carbon coefficients as the product of the annual CO_2 price per ton and the total CO_2 produced by the system, accounting for relevant product streams and demands such as electricity and treated brine.

$$\text{maximize } Annual = \lambda \cdot Profit + (1 - \lambda) \cdot Carbon\ Coefficient \tag{5}$$

$$Carbon\ Coefficient = Carbon\ Price \cdot y \tag{6}$$

To quantify CO_2 within the system, carbon coefficients are applied to the relevant streams, particularly electricity, biomass, and treated brine. The pricing associated with these streams corresponds to scenarios where CO_2 is sequestered, reflecting the carbon capture rate related to specific products and material streams. The λ-value in Equation (5) represents the weight assigned to each criterion within the objective function, which can be adjusted to identify optimal trade-offs. Different numerical values for λ were systematically selected to observe corresponding changes in profit and carbon-associated pricing. This approach, known as the weighted-sum method, effectively addresses multi-criteria optimization challenges.

The constraints of the model are as follows:

$$Ax = y \tag{7}$$

$$y_L \leq y \leq y_U \tag{8}$$

$$x \leq Mb \tag{9}$$

$$b_i \in \{0,1\} \tag{10}$$

In Equation (7), process matrix *A* considers all the inputs and outputs for each technology unit, including both materials and product streams. Equation (8) shows that the net output vector (*y*) is bounded by lower and upper limit vectors, designated by y_L and y_U, respectively. In Equation (9), an arbitrary large number *M* is multiplied to the capacity vector to allow for high upper limits. The binary variable vector *b* decides the selection of a unit. As shown in Equation (10), the variable *b* can indicate selection with a value of 1 or exclusion with 0.

2.2. The Case Study

The case study considers a polygeneration system with a desalination process that consists of five main process units. Specifically, the system includes a utility boiler, a CHP unit, an electric chiller, a ROD unit, and an EGDA unit. The CHP unit comprises an externally-fired gas turbine (EFGT) with a heat recovery steam generator for co-generation of heat [22]. EFGTs operate by keeping combustion gases separate from the turbine's moving parts, enhancing their durability and efficiency. This design enables effective use of lower-grade fuels, making EFGTs suitable for diverse biomass applications. Figure 1 depicts the superstructure of the polygeneration system with desalination, illustrating all the technologies and their respective process streams.

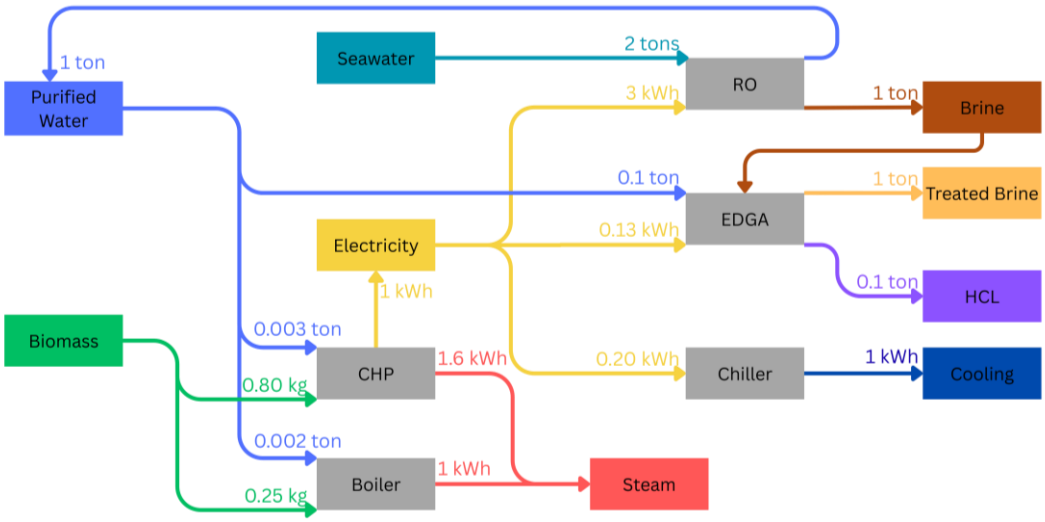

Figure 1. Superstructure of considered process units and process streams adapted with permission from Ref. [8].

The values associated with the mass and energy balance data, prices of the streams, and capital costs have been adopted from the study of Tan et al. [8]. Considering the model formulation in the previous section, the corresponding process flows are coded in the LINGO software, as represented in Appendix A. Table 1 lists process streams as rows and the process units as columns. Positive values indicate output streams while negative values indicate input streams. The values in Table 1 match the process flows in Figure 1.

Table 1. Mass and energy balance of process streams for each technology unit adapted with permission from Ref. [8].

	Utility Boiler	CHP Unit	Chiller	RO Unit	EGDA
Biomass fuel (kg)	−0.25	−0.8			
Electricity (kWh)		+1	−0.2	−3	−0.013
Steam (kWh)	+1	+1.6			
Cooling (kWh)			+1		
Purified water (t)	−0.002	−0.003		+1	−0.1
HCl (t)					+0.1
Brine (t)				+1	−1
Treated brine (t)					+1

The prices of the process streams are summarized in Table 2. While treated brine is not sold as a product, it has an associated price when CO_2 is considered. In addition, Table 2 lists upper and lower demand limits for net output. Table 3 presents the corresponding fixed capital cost and variable costs for each process unit.

Table 2. Price range and demand limits of process streams adapted with permission from Ref. [8].

	Price Range (€ per Unit)	Lower Demand Limit	Upper Demand Limit
Biomass fuel (kg)	0.20		
Electricity (kWh)	0.12	4000	10,000
Steam (kWh)	0.04	4000	12,000
Cooling (kWh)	0.06	0	1500
Purified water (t)	1.20	100	100
HCl (t)	2.40	8	8
Brine (t)	0		
Treated Brine (t)	0.73		

Table 3. Capital and operating costs of each process unit adapted with permission from Ref. [8].

	Utility Boiler	CHP Unit	Chiller	RO Unit	EGDA
Fixed Cost Component	€ 45,000	€ 380,000	€ 44,000	0	0
Variable Cost Component	€ 175/kW	€ 950/kW	€ 268/kW	€ 15,000/t	€ 350/t

3. Results and Discussion

3.1. Maximizing Profitability

A control scenario was considered where carbon-associated prices were not considered, and the only objective is to maximize profit. This corresponds to a λ-value of 1 to indicate an objective solely for profitability. Table 4 summarizes the control results. Based on the results, an annual profit of €4,691,000 can be attained when utilizing the CHP, chiller, RO, and EGDA units. Notably, the boiler was excluded, which indicates that the steam demand is handled entirely by the CHP unit, as shown in the optimized results in Figure 2. The exclusion of the boiler can be attributed to the dual output nature of the CHP unit, where it is more profitable to handle all steam demand while simultaneously generating electricity. In turn, biomass can be reallocated for other product streams, such as biofuel, bio-oils, or synthetic gas. Besides biomass, the CHP unit provides electricity to offset demand from the electricity grid, indirectly reducing carbon emissions with reduced imports. The chiller remains the only unit for the cooling demand and therefore remains in the system. Both the RO and EGDA unit operate to supply water, brine, treated brine, and HCl in the system. The positive values indicate contribution to the overall annual profit. Particularly, HCl can significantly impact results when considering possible price fluctuations, but this only applies when HCl is sold. Similarly, treated brine is the main contributor to the carbon capture of the system, which can have varying carbon-associated pricing.

Table 4. Summary of results of maximized profitability.

	Maximized Results
Profit (thousand euro/year)	4691
Boiler (kW)	0
CHP (kW)	7500
Chiller (kW)	1500
RO (t/h)	130.5
EGDA (t/h)	80

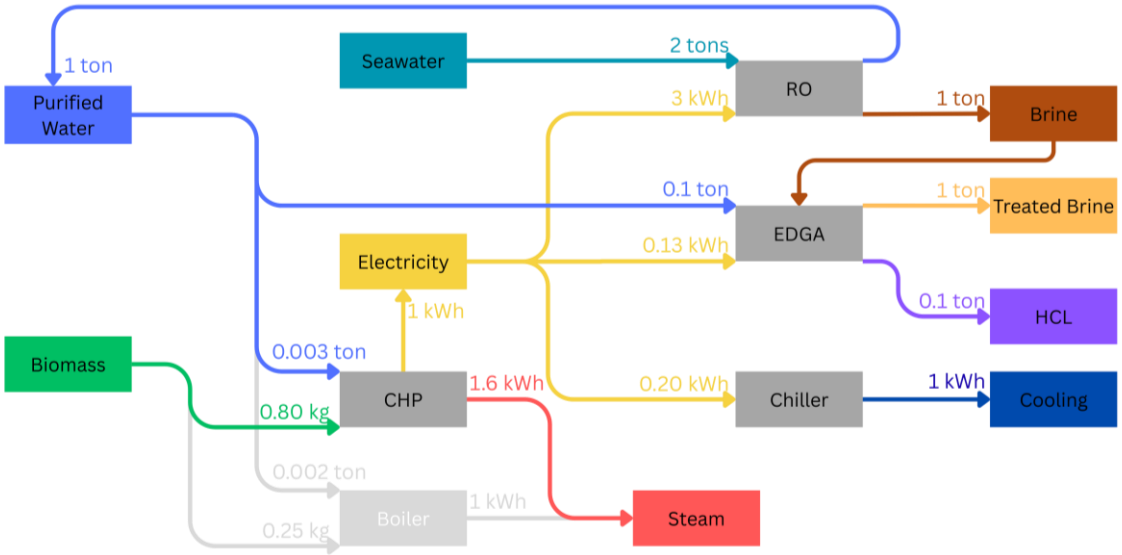

Figure 2. Superstructure of the optimized results.

3.2. Minimizing Carbon-Associated Price

Figure 3 summarizes the results when considering the annual profit and carbon-associated price. These values were obtained by varying the λ-value from 1 to 0, indicating the prioritization from maximizing profit to minimizing carbon-associated price respectively. At λ-values of 0 and 1, a profit of €447,000 per year and €4,691,000 per year are exhibited, respectively. The exact values for annual profit at each λ-value are presented in Appendix B. Regardless of the inclusion of carbon emissions, the system generates net positive profitability. Notably, the results indicate similar operating capacities for each unit, implying that the same units are used at similar capacities.

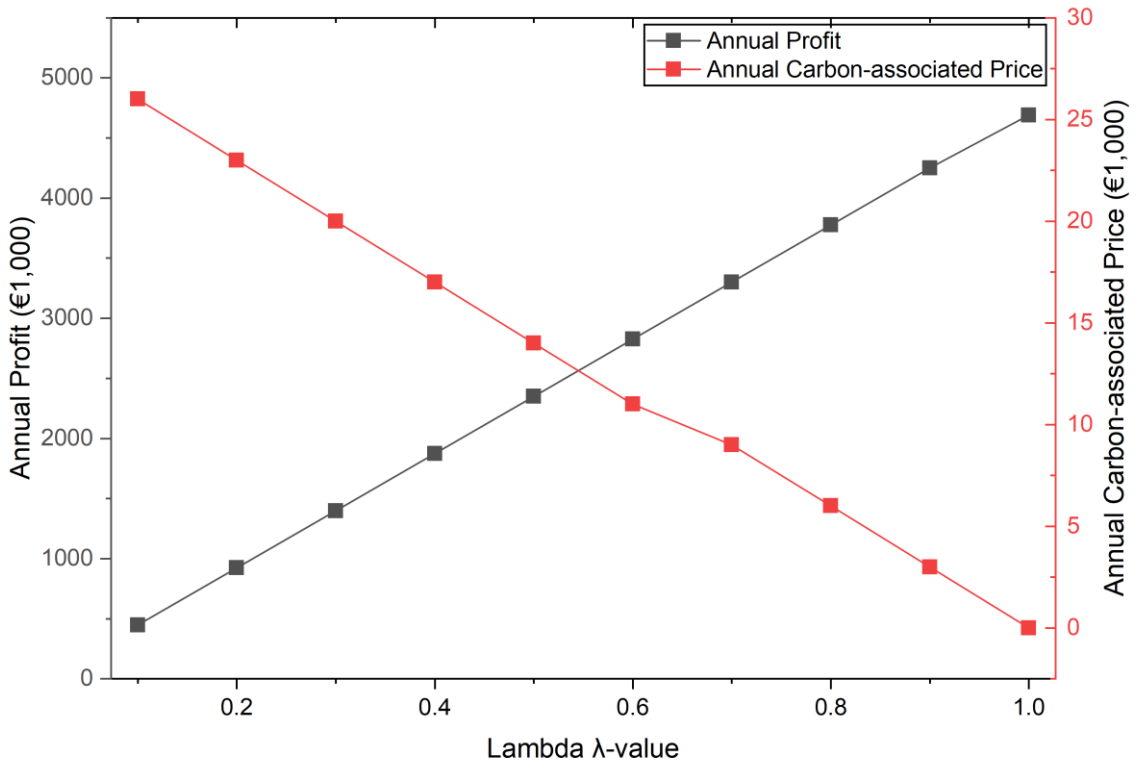

Figure 3. Variations in annual carbon-associated price and annual profit as λ increases.

Similar working capacities can be attributed to system demands, which remain constant for both cases. Throughout all scenarios, the boiler remained unchosen. For the chiller, capacity remains the same regardless of carbon-associated price as the cooling demand will not decrease and is independent of carbon-associated pricing. Likewise, the electricity demand is handled mainly by the imported electricity as well as the CHP unit, while the heating demand is handled primarily by the CHP unit. The RO and EGDA units account for treated brine as carbon capture, but there was no significant change in capacities.

The results in Figure 3 demonstrate that the carbon-associated price and profit have a linear relationship. Higher carbon-associated prices would result in lower profit yields, implying the difficulty in simultaneously maximizing profits and minimizing carbon-associated price as an objective. For this system, the linear relationship suggests that for certain profit margin, the corresponding carbon-associated price can be determined. In this study, the carbon-associated price accounts for 1.42% to 5.73% of total profitability at decreased λ-value. When carbon-associated prices are viewed as profitability losses, these percentages can be significant when paired with high upfront investment technologies. Therefore, when designing systems for profitability or carbon-associated price, this model can indicate the linear trade-off between the two criteria. For polygeneration systems aiming for negative emissions, other technologies with low-carbon emission outputs can be considered. Given this case study, a potential solution is substituting the imported grid electricity with more carbon-neutral renewable energy sources such as hydroelectric power.

The negative slope indicates that profitability will continue to decrease when considering carbon-associated prices. Based on Ibishova et al. [23], another method for assessing trade-offs between the two variables involves considering the carbon emission reduction relative to return on assets (ROA). Ibishova et al. identified the alternative energy sectors and gas, water, and multiutilities sectors with a ROA of 1.004 and 1.758, respectively, which implies a near one-to-one trade-off. The results in Figure 3 show a 0.006 slope, indicating significant room for system improvement. One method for achieving this is conducting analysis and optimization with other technologies, including NETs utilizing enhanced weathering and direct air capture.

Linear relationships between objectives have been noted in similar studies. Aviso et al. [16] integrated MILP into a polygeneration system with CO_2 removal and studied the trade-offs between annual profit and annual net CO_2 emissions against CO_2 costs per ton. When the cost of CO_2 was neglected, annual profitability was maximized at approximately $12 million per year. As cost of CO_2 increased, annual profitability decreased linearly until stabilizing at approximately $5 million per year. Trinks et al. [24] found that higher carbon efficiency is associated with higher

profitability, measured as return on assets (ROA). Specifically, the relationship is modeled as linear in the panel regression analysis, with an average 0.1 increase in carbon efficiency corresponding to about a 1.0% increase in profitability, holding other factors constant. These findings suggest that carbon-efficient production not only improves operational performance but also reduces financial risks linked to carbon regulation. Pratama et al. [25] studied biomass gasification combined-cycle plant co-producing electricity and methanol and reported a trade-off between delivering negative net carbon emissions but at significantly high capital and operating expenses.

However, non-linear relationships have also been reported in other studies. Yang and Zhang [26] studied the relationship between carbon constraints to the profitability of power plants and reported a U-shaped relationship based on theoretical and empirical results. Overcoming high initial investment costs from research and development would result in increasing profitability while decreasing long-term carbon emissions. Bartolini et al. [27] studied the trade-offs in distributed energy systems. They reported that increasing carbon pricing encourages greater adoption of renewable photovoltaic (PV) capacity, reducing emissions but only modestly affecting costs. However, lower natural gas prices can shift the optimal design toward fossil-fuel-based combined heat and power (CHP) systems, increasing primary energy consumption and potentially undermining carbon reduction goals despite carbon pricing. De Souza et al. [28] optimized a district polygeneration to minimize annual cost and CO_2. Their findings demonstrate an exponential relationship where beyond a certain emission saving, the associated cost rapidly rise. Initial emission cuts within energy communities are profitable or low-cost, but beyond an inflection point, the marginal cost rises significantly. Pinto et al. [29] developed a MILP model for a residential polygeneration microgrid which exhibited the ability to simultaneously reduce costs and CO_2 emissions. The gains in profitability and emission reduction by utilizing both renewable and storage technologies encourage synergy as opposed to trade-offs.

In this study, manipulating the model constraints to consider lower demands or lower carbon-associated price produces an infeasible solution, which would imply a rework of the model. While the reference values have been set, considering price and demand fluctuations is also important. Including a range of values may reveal more nuanced relationship between profitability and carbon-associated price.

3.3. Life Cycle Assessment (LCA) Perspective

Incorporating a ROD/IOC unit in polygeneration systems has not yet been implemented in realistic settings. Aside from the operating conditions and economic gains presented in the optimization results, the environmental impact of the technology can be assessed from its entire life cycle. The current study predominantly focuses on the environmental impacts during the operation of the system; however, optimization from purely the operation phase can shift environmental burdens to other life cycle stages or impact categories. While the current study does not conduct a life cycle assessment (LCA), there are some literatures that delve into LCA of indirect ocean capture and reverse osmosis desalination technologies. One study investigated an LCA on seawater reverse osmosis (SWRO) desalination for both potable and industrial water production [30]. By highlighting the water intake, treatments, and water management processes, the study comprehensively examines material, energy, and waste streams for each stage of the system. The LCA study reveals that electricity consumption dominates environmental impacts across most categories, contributing 91.1% and 90.1% to global warming for potable and industrial water production respectively, while brine rejection primarily drives eutrophication impacts due to ammonium and phosphorus emissions.

When conducting LCA studies for IOC and ROD technologies, the most critical system process to evaluate is energy production and consumption. One study highlighted the bipolar membrane electrodialysis which accounts for 80% of total energy use and requires carbon-free electricity to avoid net CO_2 emissions [5]. LCA should consider end-of-life processes, maintenance cycles, and the integration of multiple product streams, including captured CO_2, fresh water, and electricity, to determine if the environmental benefits outweigh the lifecycle costs of energy-intensive but potentially low-cost, from 15 to 35 euros per ton CO_2, integrated system [31].

4. Conclusions

This paper introduces weighted criteria in the optimization of a polygeneration system with ROD/IOC technology unit. The MILP model investigated maximizing profit while also minimizing carbon-associated price. The optimized operating conditions are as follows: the CHP at 7500 kWh, chiller at 1500 kWh, RO unit at 130.5 tons per hour, EDGA unit at 80 tons per hour, and boiler at 0 kWh. The results indicate a direct link between carbon-associated price and profitability, where the trade-off has an inverse linear behavior. At maximized profit, profitability reaches €4,691,000 per year, while at minimum profit, profitability is €447,000 per year. Carbon-associated price accounts for 1.42% to 5.73% of the profit at decreased λ-values. Thus, when designing a polygeneration system, it is

important to define the target carbon-associated price and profitability. However, the results presented are specific to this case study, and further optimization can be conducted to adjust parameters according to requirements of the plant facilities. To improve the robustness of the model, a sensitivity analysis can be performed for uncertainties in parameters, such as price and demand fluctuations.

Future work may focus on integrating renewable energy sources such as hydroelectric power to further reduce emissions from imported electricity streams and encourage self-sufficient systems. In terms of optimization, further studies can investigate multi-objective optimization that considers time variations during system operation. Such research could identify the optimal capacities and their corresponding carbon emissions as the electricity, heating, and cooling demands fluctuate, improving both efficiency in meeting demands and reducing carbon emissions.

Author Contributions: M.C.O.M.: conceptualization, methodology, investigation, formal analysis, writing—original draft; A.T.U.: conceptualization, formal analysis, writing—original draft

Funding: This research received no external funding.

Data Availability Statement: Data will be made available on request.

Conflicts of Interest: The authors declare no conflict of interest.

Nomenclature

$Annual\ Profit$	actual annual profitability
	ideal annual profitability
NSV	net stream revenue
ACC	annualized capital and operational costs
$Carbon\ Coefficient$	carbon-associated price
$Carbon\ Price$	carbon coefficients that relate tons of carbon to price
AF	annualizing factor
AWH	annual operating hours
A	process matrix
c_1	price vector
c_2	variable cost vector
c_3	fixed cost vector
M	arbitrary large number
y_L	net output lower limit vector
y_U	net output upper limit vector
b_i	binary variable vector for i technology unit
x	capacity vector
y	net output vector

Appendix A. MILP Code

```
max = annual; !lambda = 0.1;
annual = 0.1*(profit) + 0.9*(carbon);
@free(fnsv);@free(facc);@free(carbon);

profit = fnsv - facc;
fnsv = 8000*(0.12*y1 +0.04*y2 +0.06*y3 +1.2*y4 +2.4*y5 +0*y6 +0.73*y7 +0.2*y8);
facc = 0.8*(capex_fix + capex_var);

capex_fix = 45000*z1 +380000*z2 +44000*z3 +0*z4 +0*z5;
capex_var = 175*x1 +950*x2 +268*x3 +15000*x4 +350*x5;

carbon = 100*(0.0073*y7 - 0.0168*y1 - 0.038*y2); carbon < 7585.32;

!Energy balance;
+0*x1      +1*x2      -0.2*x3    -3*x4      -0.013*x5   = y1; !Electricity (kWh);     4000 < y1; y1 < 10000; !y1=24000;
+1*x1      +1.6*x2    +0*x3      +0*x4      +0*x5       = y2; !Steam (kWh);           4000 < y2; y2 < 12000; !y2=48000;
+0*x1      +0*x2      +1*x3      +0*x4      +0*x5       = y3; !Cooling (kWh);         0 < y3; y3 < 1500; !y3=9000;

!Mass balance;
-0.002*x1  -0.003*x2  +0*x3      +1*x4      -0.1*x5     = y4; !Purified water (t/h);  y4 = 100;
+0*x1      +0*x2      +0*x3      +0*x4      +0.1*x5     = y5; !HCl (t/h);             y5 = 8;
+0*x1      +0*x2      +0*x3      +1*x4      -1*x5       = y6; !Brine (t/h);
+0*x1      +0*x2      +0*x3      +0*x4      +1*x5       = y7; !Treated Brine (t/h);
-0.25*x1   +0*x2      +0*x3      +0*x4      +0*x5       = y8; !Biomass fuel (kg);

!Binary specification;
!process units;              !Capacity limits for units;
@bin(z1);                    x1 < 1000000*z1;
@bin(z2);                    x2 < 1000000*z2;
@bin(z3);                    x3 < 1000000*z3;
@bin(z4);                    x4 < 1000000*z4;
@bin(z5);                    x5 < 1000000*z5;
```

Appendix B. Computational Data for Varying Lambda

Lambda λ-Value	Profit (in Thousand Euro/Year)	Carbon Price (in Thousand Euro/Year)
1.00	4691	0
0.90	4251	3
0.80	3776	6
0.70	3300	9
0.60	2825	11
0.50	2349	14
0.40	1874	17
0.30	1398	20
0.20	923	23
0.10	447	26

References

1. Ritchie, H.; Roser, M. CO_2 emissions. Our World in Data. 2024. Available online: https://ourworldindata.org/co2-emissions (accessed on 26 April 2025).
2. NASA. *Carbon Dioxide*. 2025. Available online: https://climate.nasa.gov/vital-signs/carbon-dioxide (accessed on 26 April 2025).
3. International Energy Agency. *Renewables 2024*. 2024. Available online: https://www.iea.org/reports/renewables-2024 (accessed on 26 April 2025).
4. Haszeldine, R.S.; Flude, S.; Johnson, G.; Scott, V. Negative emissions technologies and carbon capture and storage to achieve the Paris Agreement commitments. *Philos. Trans. R. Soc. A Math. Phys. Eng. Sci.* **2018**, *376*, 20160447. https://doi.org/10.1098/rsta.2016.0447.
5. de Lannoy, C.-F.; Eisaman, M.D.; Jose, A.; Karnitz, S.D.; DeVaul, R.W.; Hannun, K. Indirect ocean capture of atmospheric CO_2: Part I. Prototype of a negative emissions technology. *Int. J. Greenh. Gas Control* **2018**, *70*, 243–253. https://doi.org/10.1016/j.ijggc.2017.10.007.
6. Eisaman, M.D.; Rivest JL, B.; Karnitz, S.D.; de Lannoy, C.-F.; Jose, A.; DeVaul, R.W.; Hannun, K. Indirect ocean capture of atmospheric CO_2: Part II. Understanding the cost of negative emissions. *Int. J. Greenh. Gas Control* **2018**, *70*, 254–261. https://doi.org/10.1016/j.ijggc.2018.02.020.
7. Davies, P.A.; Yuan, Q.; de Richter, R. Desalination as a negative emissions technology. *Environ. Sci. Water Res. Technol.* **2018**, *4*, 839–850. https://doi.org/10.1039/C7EW00502D.
8. Tan, R.R.; Aviso, K.B.; Foo DC, Y.; Lee, J.-Y.; Ubando, A.T. Optimal synthesis of negative emissions polygeneration systems with desalination. *Energy* **2019**, *187*, 115953. https://doi.org/10.1016/j.energy.2019.115953.
9. Shahabuddin, M.; Alim, M.A.; Alam, T.; Mofijur, M.; Ahmed, S.F.; Perkins, G. A critical review on the development and challenges of concentrated solar power technologies. *Sustain. Energy Technol. Assess.* **2021**, *47*, 101434. https://doi.org/10.1016/j.seta.2021.101434.
10. Luo, J.; Zhu, Q.; Morosuk, T. Advanced Exergy-Based Optimization of a Polygeneration System with CO_2 as Working Fluid. *Entropy* **2024**, *26*, 886. https://doi.org/10.3390/e26100886.
11. Lainfiesta, M.; Zhang, X.; Wu, J.; Song, H. Developing a Decision Support System for the Optimal Operating Strategies of a Polygeneration Facility. In Proceedings of the 2019 IEEE Innovative Smart Grid Technologies—Asia (ISGT Asia), Chengdu, China, 21–24 May 2019. https://doi.org/ 10.1109/ISGT-Asia.2019.8881736.
12. Fachrizal, R.; Shepero, M.; van der Meer, D.; Munkhammar, J.; Widén, J. Smart charging of electric vehicles considering photovoltaic power production and electricity consumption: A review. *eTransportation* **2020**, *4*, 100056. https://doi.org/ 10.1016/j.etran.2020.100056.
13. Urbanucci, L. Limits and potentials of Mixed Integer Linear Programming methods for optimization of polygeneration energy systems. *Energy Procedia* **2018**, *148*, 1199–1205. https://doi.org/10.1016/j.egypro.2018.08.021.
14. Aviso, K.B.; Sy, C.L.; Tan, R.R.; Ubando, A.T. Fuzzy optimization of carbon management networks based on direct and indirect biomass co-firing. *Renew. Sustain. Energy Rev.* **2020**, *132*, 110035. https://doi.org/10.1016/j.rser.2020.110035.
15. Belmonte, B.A.; Benjamin MF, D.; Tan, R.R. Optimization-based decision support methodology for the synthesis of negative-emissions biochar systems. *Sustain. Prod. Consum.* **2019**, *19*, 105–116. https://doi.org/10.1016/ j.spc.2019.03.008.
16. Aviso, K.B.; Belmonte, B.A.; Benjamin MF, D.; Jia, X.; Zhang, Y.; Tan, R.R. Optimal Integration of Polygeneration with Carbon Dioxide Removal. *Chem. Eng. Trans.* **2022**, *94*, 385–390. https://doi.org/10.3303/CET2294064.
17. Kaim, A.; Cord, A.; Volk, M. A review of multi-criteria optimization techniques for agricultural land use allocation. *Environ. Model. Softw.* **2018**, *105*, 79–93. https://doi.org/10.1016/j.envsoft.2018.03.031.

18. Olabi, V.; Alhajeri, A.; Jouhara, H. Designing a sustainable hydrogen supply chain network in the Gulf Cooperation Council (GCC) region: Multi-objective optimisation using a Kuwait case-study. *Int. J. Hydrogen Energy* **2025**, *142*, 994–1013. https://doi.org/10.1016/j.ijhydene.2025.03.296.
19. Cheng, J.; Cheng, J.; Lin, Y.; Lu, S.; Wu, P. MILP models and effective heuristic for energy-aware parallel machine scheduling with shared manufacturing. *Expert Syst. Appl.* **2025**, *271*, 126681. https://doi.org/10.1016/j.eswa.2025.126681.
20. Yilmaz, H.; Yagmahan, B. Optimization of the electric vehicle charging strategy problem for sustainable intercity travels with multiple refueling stops. *Sustain. Energy Grids Netw.* **2024**, *40*, 101546. https://doi.org/10.1016/j.segan.2024.101546.
21. Grossmann, I.E.; Santibanez, J. Applications of mixed-integer linear programming in process synthesis. *Comput. Chem. Eng.* **1980**, *4*, 205–214. https://doi.org/10.1016/0098-1354(80)85001-0.
22. Al-attab, K.A.; Zainal, Z.A. Externally fired gas turbine technology: A review. *Appl. Energy* **2015**, *138*, 474–487. https://doi.org/10.1016/j.apenergy.2014.10.049.
23. Ibishova, B.; Misund, B.; Tveterås, R. Driving green: Financial benefits of carbon emission reduction in companies. *Int. Rev. Financ. Anal.* **2024**, *96*, 103757. https://doi.org/10.1016/j.irfa.2024.103757.
24. Trinks, A.; Mulder, M.; Scholtens, B. An Efficiency Perspective on Carbon Emissions and Financial Performance. *Ecol. Econ.* **2020**, *175*, 106632. https://doi.org/10.1016/j.ecolecon.2020.106632.
25. Pratama, M.R.; Muthia, R.; Purwanto, W.W. Techno-economic and life cycle assessment of the integration of bioenergy with carbon capture and storage in the polygeneration system (BECCS-PS) for producing green electricity and methanol. *Carbon Neutrality* **2023**, *2*, 26. https://doi.org/10.1007/s43979-023-00069-1.
26. Yang, S.; Zhang, X. Study on the U-shaped relationship of carbon constraint on the large thermal power plants' profitability. *Nat. Hazards* **2017**, *89*, 1421–1435. https://doi.org/10.1007/s11069-017-3028-7.
27. Bartolini, A.; Mazzoni, S.; Comodi, G.; Romagnoli, A. Impact of carbon pricing on distributed energy systems planning. *Appl. Energy* **2023**, *301*, 117324. https://doi.org/10.1016/j.apenergy.2021.117324.
28. De Souza, R.J.; Reini, M.; Serra, L.M.; Lozano, M.A.; Nadalon, E.; Casisi, M. Multi-Objective Optimization of an Energy Community Powered by a Distributed Polygeneration System. *Energies* **2024**, *17*, 3085. https://doi.org/10.3390/en17133085.
29. Pinto, E.S.; Serra, L.M.; Lázaro, A. Energy communities approach applied to optimize polygeneration systems in residential buildings: Case study in Zaragoza, Spain. *Sustain. Cities Soc.* **2022**, *82*, 103885. https://doi.org/10.1016/j.scs.2022.103885.
30. Fayyaz, S.; Masjedi, S.K.; Kazemi, A.; Kahki, E.; Moeinaddini, M.; Olsen, S.I. Life cycle assessment of reverse osmosis for high-salinity seawater desalination process: Potable and industrial water production. *J. Clean. Prod.* **2023**, *382*, 135299. https://doi.org/10.1016/j.jclepro.2022.135299.
31. Straatman, P.J.T.; van Sark, W.G.J.H.M. Indirect air CO_2 capture and refinement based on OTEC seawater outgassing. *iScience* **2021**, *24*, 102754. https://doi.org/10.1016/j.isci.2021.102754.